Control of Reactivity of Dinuclear Nickel(II) Amine-Thiolate Complexes

Berthold Kersting[a]

Keywords: Septadentate N_5S_2-ligand / Dinuclear complexes / Nickel / Reactivity / Redox chemistry

The coordination chemistry of a series of dinickel complexes of the new septadentate amine-thiolate ligand *N*,*N*′-bis[2-thio-3-aminomethyl-5-*tert*-butylbenzyl]diethylenetriamine, H_2**9**, has been investigated in the context of ligand binding and oxidation state changes. The complexes $[Ni_2(\mathbf{9})(L)][ClO_4]_2$ (**10**), $[Ni_2(\mathbf{9})(Cl)][Cl]$ (**11**), $[Ni_2(\mathbf{9})(L)][BPh_4]_2$ (**12**), and $[Ni_2(\mathbf{9})(NCS)][OH{\cdot}OH_2]$ (**13**) have central $N_2Ni(\mu\text{-}SR)_2NiN'_3L$ cores [L = labile solvent molecule (**10**, **12**), Cl^- (**11**), and NCS^- (**13**)] composed of dithiolate bridged planar NiN_2S_2 and six-coordinate NiN'_3S_2L units. This is demonstrated for **11** and **13** by crystal structure determinations and for **10** and **12** by UV/Vis spectroscopy and room temperature magnetic susceptibility measurements. Complexes **10**, **11**, or **12** readily add other co-ligands at the NiN'_3S_2L fragment by substitution of the solvent molecule L (**10**, **12**) or the chloride substituent (**11**). The overall structure of the parent complexes is not affected by the substitution reactions. An electrochemical study has shown that complex **10** undergoes two successive one-electron oxidations at +0.88 and +0.41 V vs SCE. The oxidized species are not thermally stable, but electronic absorption spectra and EPR spectra are indicative of the presence of Ni^{III} species.

Introduction

Polydentate Schiff base ligands derived from 2,6-diformyl-4-methylthiophenol and certain α,ω-diamines are versatile ligands in the preparation of discrete dithiolate-bridged dimetal complexes.[1] Their specific coordination mode is due to the presence of *o*,*o*′-iminomethyl substituents, which, by formation of intramolecular chelate rings, effectively block terminal metal-coordination sites and, in contrast to a variety of monodentate thiolate ligands, allow for a better control of the nuclearity and reactivity of transition metal thiolate complexes.[2] Due to the presence of the soft thiolate ligands it is also often possible to stabilize metal ions in unusually high oxidation states. The coordination chemistry of such ligands, in particular with first-row transition metals M = Fe, Ni, and Cu,[3–5] has thus been an area of considerable interest recently, since dithiolate bridged, redoxactive $M(\mu\text{-}SR)_2M$ assemblies also occur in the active sites of various enzymes.[6–8] Surprisingly, there is a paucity of information in the literature concerning the chemistry of the analogous amine-thiophenolate ligands,[9][10] although their corresponding complexes offer the further advantage of being hydrolytically more stable.[11]

Recently we reported the synthesis and characterization of coordinatively unsaturated dinuclear nickel amine-thiolate complexes $[Ni_2(\mathbf{1})_2]^{2+}$ (**2**)[12] and $[Ni_2(\mathbf{4})]^{2+}$ (**5**) (Scheme 1).[13] Both complexes exhibit $N_2Ni(\mu\text{-}SR)_2NiN_2$ core structures and both were found to readily add co-ligands resulting in total or partial change of nickel coordination numbers from four in the parent complexes (**2**, **5**) to six in the products (**3**, **6**). While the former transformation (**2** → **3**) is accompanied by severe metal/ligand donor atom rearrangements, the latter (**5** → **6**) leaves the overall core structure of the parent complex unchanged, which is due to its fixation by the hexadentate ligand. This situation, along with the (slightly) different nickel coordination environments in **3**, means that its reactions with monodentate co-ligands proceed in a well-defined manner. Scheme 2 depicts the stereochemical courses of these reactions.

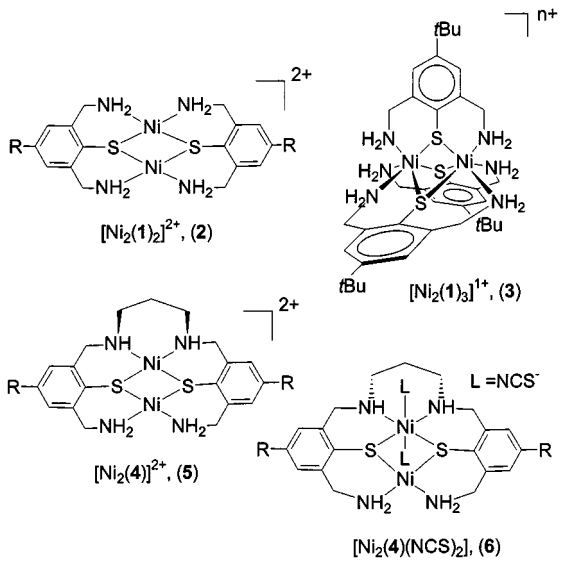

Scheme 1. Structures of dinuclear nickel amine-thiolate complexes **2**,[12] **3**,[12] **5**,[13] and **6**[13]

To further explore the reactivity of thiolate-bridged complexes featuring a central $Ni(\mu\text{-}SR)_2Ni$ core, we have now focused on the reactivity of nickel complexes of the amine-thiolate ligand H_2**9** (see Scheme 2), which provides dissimilar N_2S_2 and N'_3S_2 donor sets (N and N′ denote primary

[a] Institut für Anorganische und Analytische Chemie,
Universität Freiburg,
Albertstrasse 21, D-79104 Freiburg, Germany
Fax: (internat.) + 49(0)761/203-6001
E-mail: kerstber@sun2.ruf.uni-freiburg.de

  1434–1948/99/1212–2157 $ 17.50+.50/0

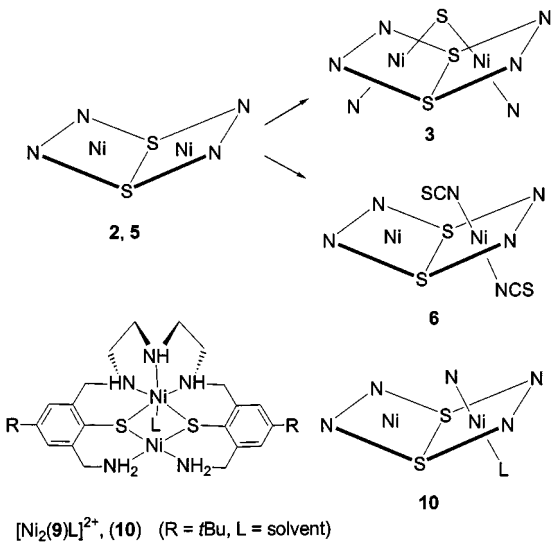

Scheme 2. Core structural changes during transformations **2** → **3** and **5** → **6** and structure of dinuclear nickel complexes of amine-thiolate ligand H_2**9**

and secondary nitrogen atoms, respectively). It was assumed that the $-(CH_2)_2NH(CH_2)_2-$ chain bridging the two 2,6-bis(aminomethyl)-4-*tert*-butylthiophenol units would not distort the typical coordination observed in complexes **2** and **5**. Instead, the additional NH donor atom was anticipated to be involved in a specific *fac* coordination mode with two other secondary nitrogen and two bridging thiolate sulfur atoms, thereby yielding a six-coordinate $NiS_2N'_3L$ unit with a weakly bound solvent molecule L at the sixth coordination site. Similar strategies have been used by Sellmann et al. to control the reactivity of octahedral $MN_{5-x}S_xL$ complexes.[14]

This paper reports the synthesis of H_2**9** and some of its dinickel complexes. The crystal structures of $[Ni_2(\mathbf{9})(Cl)][Cl]$ (**11**) and of the isothiocyanate complex $[Ni_2(\mathbf{9})(NCS)][OH{\cdot}OH_2]$ (**13**), which is obtained by reaction of **11** with NH_4SCN, are also presented. The results obtained clearly demonstrate that control of the reactivity of dinuclear amine-thiolate complexes is possible, given that their core structures are assembled by specific, polydentate amine-thiolate ligands. All complexes have been further characterized by IR and UV/Vis spectroscopy and by cyclic voltammetry. Products obtained by chemical oxidation of the thiolate complexes have been characterized by UV/Vis and EPR spectroscopy.

Results and Discussion

Ligand Synthesis

The heptadentate N_5S_2 ligand, H_2**9**, was prepared following the method described in Scheme 3. In the first step, two equivalents of aldehyde **7** were condensed with one equivalent of *N*,*N*-bis(2-aminoethyl)amine. The resulting imine/thioether/oxime compound was reduced in situ with $NaBH_4$ to give the corresponding amine/thioether/oxime compound **8**. Treatment of **8** with sodium in liquid ammonia resulted in reduction of the oxime groups and reductive cleavage of the ArS−*t*Bu bonds to give, after acidic workup, the pentahydrochloride salt, $H_2\mathbf{9} \cdot 5\,HCl$, in an over-all yield of 56%. $H_2\mathbf{9} \cdot 5\,HCl$ is very soluble in protic solvents such as water or methanol. These solutions can be handled in air for short periods of time. They were, however, freshly prepared under an inert atmosphere for the synthesis of the metal complexes.

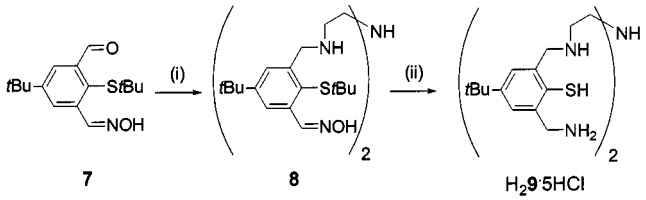

Scheme 3. Preparation of $H_2\mathbf{9} \cdot 5\,HCl$: (*i*) 0.5 equiv. $NH(CH_2CH_2NH_2)_2$, $NaBH_4$; (*ii*) Na/NH_3, HCl

Synthesis of Dinuclear Nickel Complexes

The preparations and notations of dinuclear nickel complexes of the heptadentate amine-thiolate ligand are summarized in Scheme 4. Ligand $H_2\mathbf{9} \cdot 5\,HCl$ reacted with $Ni(ClO_4)_2 \cdot 6\,H_2O$ or $NiCl_2 \cdot 6\,H_2O$ in the presence of a base such as NEt_3 in 1:2:7 molar ratios to give complexes $[Ni_2(\mathbf{9})(L)][ClO_4]_2$ (**10**) and $[Ni_2(\mathbf{9})(Cl)][Cl]$ (**11**), respectively, as red microcrystalline solids. Addition of $NaBPh_4$ to a solution of **10** in MeOH produced complex $[Ni_2(\mathbf{9})(L)][BPh_4]_2$ (**12**) in good yield. The formulation of complexes **10**, **11**, and **12** as dinuclear complexes was confirmed by X-ray crystal structure determination of **11** (see below). In contrast to **10** and **11**, the tetraphenylborate salt **12** was found to exhibit good solubility in solvents such as acetonitrile or dichloromethane, thus facilitating spectroscopic studies of the $[Ni_2(\mathbf{9})(L)]^{2+}$ complex in noncoordinating solvents (see below).

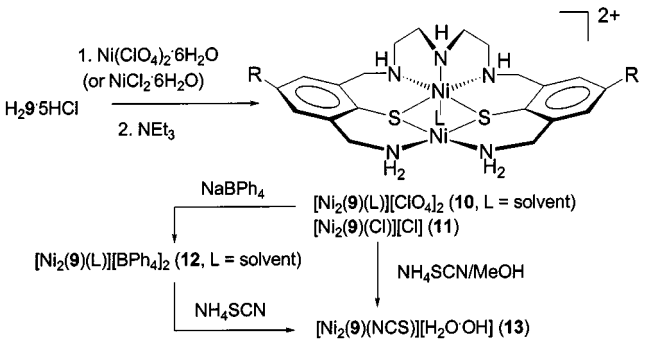

Scheme 4. Preparation of nickel complexes **10**−**13**

Reaction of complexes **10** or **11** with ammonium thiocyanate in an acetonitrile/methanol mixed solvent system resulted in the precipitation of a dark-red crystalline mate-

rial that was shown by analysis to be $[Ni_2(\mathbf{9})(NCS)][OH{\cdot}OH_2]$ (**13**). This complex could be obtained independently by reaction of the tetraphenylborate complex **12** with NH_4SCN in the same solvent system. Once precipitated, complex **13** redissolves in *N*,*N*-dimethylformamide only. Interestingly, complex **13** showed no tendency to bind further NCS^- ions − even in the presence of a 10-fold molar excess of NH_4SCN.

Complexes **10** (μ_{eff} = 3.1 μ_B), **11** (μ_{eff} = 3.1 μ_B), **12** (μ_{eff} = 3.0 μ_B), and **13** (μ_{eff} = 3.1 μ_B) are all paramagnetic in the solid state at 295 K, implying that the complexes are all composed of a planar, diamagnetic $Ni^{II}N_2S_2$ (S = 0) unit and an octahedral, paramagnetic $Ni^{II}N'_3S_2L$ center (S = 1) per molecule of complex. The presence of a six-coordinate Ni^{II} ion was confirmed for **11** and **13** by X-ray crystal structure determinations, and for **10** and **12** by electronic absorption spectroscopy (see below). In the solid state, the nature of the substituent L for complexes **10** and **12** could not be unambiguously identified. Possible candidates for L are a methanol or a water molecule.

IR spectra of **10** and **12** are very similar except for the absorptions of the anions. The ν(ClO) stretching frequency of the ClO_4^- ions in **10**, for example, is split into three very strong and sharp absorptions at 1150, 1115, and 1089 cm^{-1}. From the splitting one might conclude that a ClO_4^- ion occupies the free coordination site L in **10**. However, in $[Ni_2(\mathbf{4})][ClO_4]_2$ (**5**)[13] where a similar splitting of the $\nu_3(F_2)$ mode is observed, the ClO_4^- ions are not involved in coordination to the nickel ions. The splitting of this band might thus be caused by hydrogen bonding interactions with NH groups of the ligand. Unfortunately, it was not possible from the IR data to identify the nature of the substituent L in **10** and **12**.

Compound **13** was shown by infrared spectroscopy to contain no ClO_4^- (absence of the characteristic Cl−O stretching frequency at 1100 cm^{-1}). A new feature at 2090 cm^{-1} [ν(CN)] revealed the presence of a thiocyanate ion. Relative to the ν(CN) stretching frequency of KSCN (2053 cm^{-1}), the shift to higher frequencies implied coordination of the thiocyanate ion.[15]

Crystal Structures of 11 and 13

The X-ray crystal structure determinations of amine-thiolate complexes **11** and **13** confirm the dinuclear nature of the amine-thiolate complexes. They also demonstrate that the substitution reactions do not affect the overall structures of the parent complexes, which is in contrast to the severe ligand/donor atom rearrangements observed in the core structures during reactions of complexes **2** and **5**. The structures of the complexes are displayed in Figures 1 and 2 together with the atomic numbering schemes.

Complex **11** is composed of the dinuclear complex $[Ni_2(\mathbf{9})(Cl)]^+$, one water and two acetonitrile molecules of crystallization, and a chloride ion. Both the water molecule and the chloride ion are involved in hydrogen bonding interactions with the hydrogen atoms of nitrogen atoms N(1), N(3), and N(5) of the complex monocation. The corresponding distances are summarized in the legend to Figure 3. There are no bonding interactions between the chloride ion and the nickel atoms of the cation. The shortest distance is 3.783(3) Å for Cl(2)···Ni(2). A similar hydrogen bonding network is observed in complex **13**, where the Cl^- ion is replaced by an OH^- ion (see below).

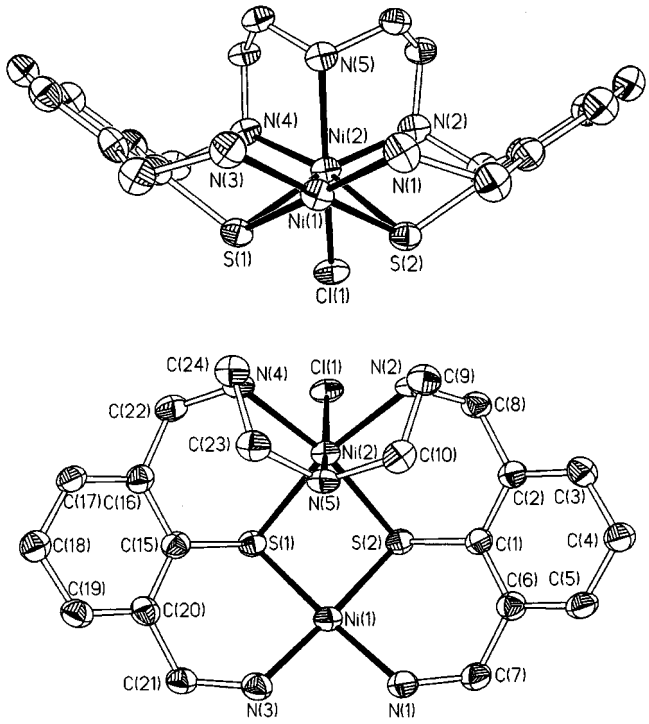

Figure 1. Molecular structure and atomic numbering of the $[Ni_2(\mathbf{9})(Cl)]^+$ cation in **11** (50% probability thermal ellipsoids). For clarity, *tert*-butyl groups and hydrogen atoms have been omitted

Table 1. Selected bond lengths [Å] in **11** and **13**

	11	**13**		**11**	**13**
Ni(1)−S(1)	2.200(2)	2.196(1)	Ni(2)−S(1)	2.414(2)	2.425(2)
Ni(1)−S(2)	2.189(2)	2.203(2)	Ni(2)−S(2)	2.429(2)	2.480(1)
Ni(1)−N(1)	1.954(4)	1.928(4)	Ni(2)−N(2)	2.090(4)	2.097(4)
Ni(1)−N(3)	1.943(4)	1.946(5)	Ni(2)−N(4)	2.095(4)	2.110(4)
			Ni(2)−N(5)	2.134(4)	2.147(4)
Ni(1)···Ni(2)	3.103(1)	3.149(1)	Ni(2)−L[a]	2.490(2)	2.070(5)

[a] L = Cl(1) in **11**, L = N(6) (NCS) in **13**.

The $[Ni_2(\mathbf{9})(Cl)]^+$ cation possesses an idealized C_s symmetry with a pseudo-mirror plane passing through the two nickel atoms and the secondary nitrogen atom N(5). Its overall structure is very similar to that of the neutral complex $[Ni_2(\mathbf{4})(NCS)_2]$ (**6**, see Scheme 1), from which it may be derived by replacing one NCS^- ion with the nitrogen atom N(5) of the lateral bis(2-aminoethyl)amine moiety. The average Ni−N and Ni−S bond lengths for the planar NiN_2S_2 (1.949 Å and 2.195 Å) and six-coordinate NiN_3S_2Cl sites (2.106 Å and 2.422 Å) show no unusual features and compare well with those in other planar NiN_2S_2[16] and octahedral NiN_4S_2 complexes,[13][17] respec-

tively. The Ni(2)−Cl(1) distance of 2.490(2) Å is likewise found in a range typical for six-coordinate NiN_xS_yCl complexes.[18] It should be noted that the Ni(2)−N(5) bond length of 2.134(4) Å *trans* to Ni(2)−Cl(1) is significantly longer than the other two Ni(2)−N distances. This bond length and the angle N(5)−Ni(2)−Cl(1) [162.9(1)°] imply that the N_3S_2 binding pocket of the ligand is too small to accommodate a nickel(II) ion in a regular octahedral coordination. The same conclusions can be drawn from the structure of **13**.

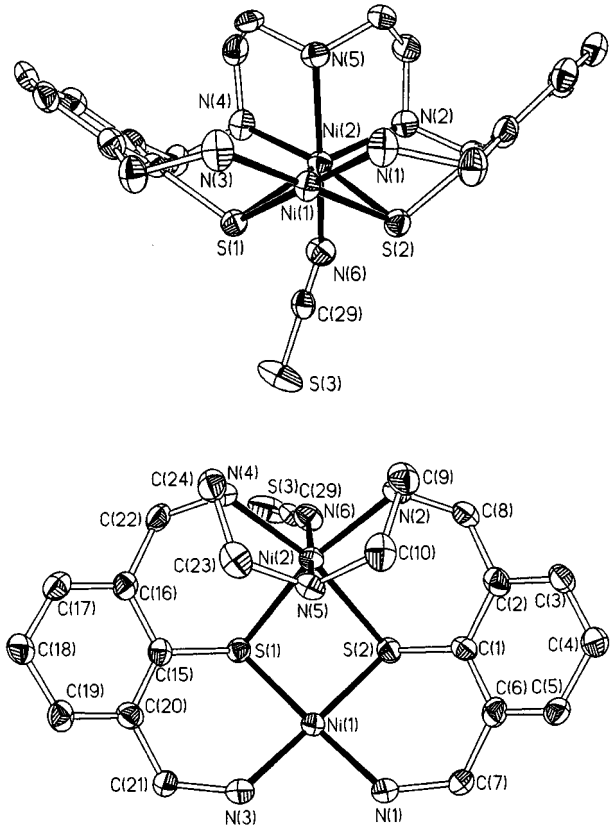

Figure 2. Molecular structure and atomic numbering of the $[Ni_2(\mathbf{9})(NCS)]^+$ cation in **13** (50% probability thermal ellipsoids). For clarity, *tert*-butyl groups and hydrogen atoms have been omitted

The isothiocyanate complex **13** is composed of the dinuclear complex $[Ni_2(\mathbf{9})(NCS)]^+$, a water molecule of crystallization, and a hydroxide ion. The hydroxide ion forms a strong $H_2O\cdots H-O$ hydrogen bonding contact to the water solvent molecule [$H_2O(1)\cdots O(2)$ 2.782(7) Å]. It should be noted that this structure is different from the $HO\cdots H\cdots OH^-$ arrangement generally found in hydrated hydroxy complexes of metals.[19] The formation of the present structure may arise from the three additional $HO^-\cdots H-N$ hydrogen bonding interactions with nitrogen atoms N(1), N(3), and N(5) of the complex monocation [O(1)···N(1) 3.239(7) Å, O(1)···N(3) 3.355(6) Å, O(1)···N(5) 3.222(7) Å]. In a similar way to **11**, there are no bonding interactions between the hydroxo or water oxygen atoms and the nickel ions of the cation. The shortest distance is 3.632(3) Å for O(1)···Ni(1). The structure of the $[Ni_2(\mathbf{9})(NCS)]^+$ cation may be simply

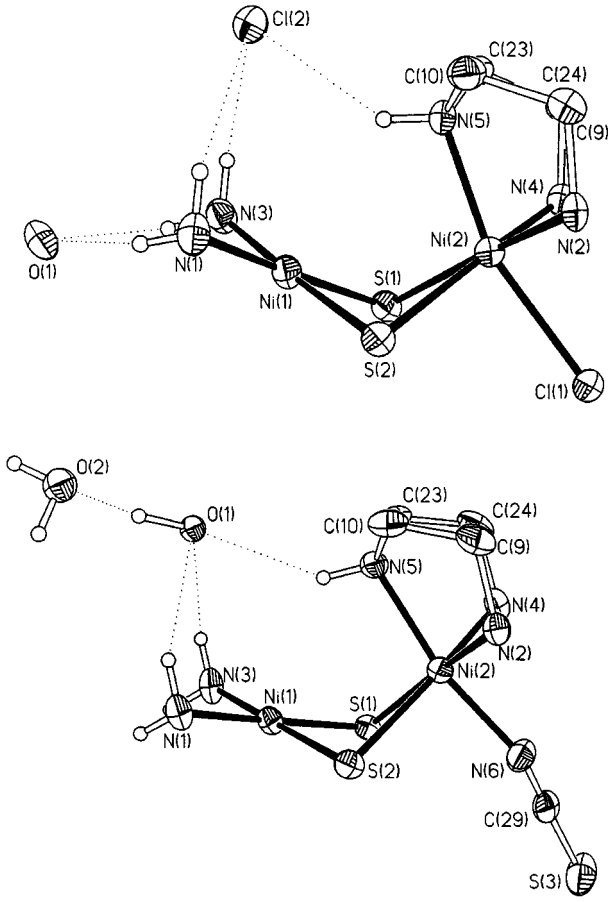

Figure 3. Core structures of complexes **11** and **13** (50% probability thermal ellipsoids). Hydrogen bonding interactions [A] in **11**: Cl(1)···N(1) 3.436(8), Cl(1)···N(3) 3.301(9), Cl(1)···N(5) 3.250(8), O(1)···N(1) 3.084(7), O(1)···N(3) 2.927(6), and in **13**: O(1)···O(2) 2.782(7), O(1)···N(1) 3.239(7), O(1)···N(3) 3.355(6), O(1)···N(5) 3.222(7). N−S and C−S bond lengths in **13**: N(6)−C(29) 1.160(7), S(3)−C(29) 1.629(6)

derived from that of $[Ni_2(\mathbf{9})(Cl)]^+$ by replacing the chloro ligand with an isothiocyanate group. There are no other gross structural changes, as evidenced by the similar shapes and similar Ni−N and Ni−S bond lengths (see Table 1).

The main difference between **5** and the complexes of the present study is the number of co-ligands that can be coordinated to the dinickel site. Dicationic **5** binds two NCS^- ligands to give complexes of the type $[N_2Ni(\mu\text{-}SR)_2NiN'_2(NCS)_2]$ (**6**) with the co-ligands in *trans* positions at the octahedral $S_2NiN'_2(NCS)_2$ site. This core structure is already partially preassembled in **10**, **11**, or **12** with an exchangeable substituent L and a nonexchangeable NH donor in place of the NCS^- ions in **5**. Hence the complexes of the present study bind only one co-ligand.

Electronic Absorption Spectra of Nickel Complexes 10−13

Although structural data for complexes **10** and **12** are currently not available, both are assumed to have a central $N_2Ni(\mu\text{-}SR)_2NiN'_3(L)$ core similar to that found for com-

Table 2. Electronic absorption spectral data for dinuclear nickel-amine-thiolate complexes

complex	solvent	donor set[a]	λ_{max} (nm) [ε ($M^{-1}cm^{-1}$)]
divalent nickel complexes			
$[Ni_2(\mathbf{1})_2]^{2+}$ (**2**)	CH_3CN	$2 \times N_2S_2$	503 (1049)
$[Ni_2(\mathbf{1})_3]^{1+}$ (**3**)	DMF	$2 \times N_3S_3$	593 (177), 922 (113), 1024 (103)[12]
$[Ni_2(\mathbf{4})]^{2+}$ (**5**)	CH_3CN	N_2S_2, N'_2S_2	501 (1005)[13]
$[Ni_2(\mathbf{9})L]^{2+}$ (**10**)	MeOH	N_2S_2, N'_3S_2L	518 (416), 624sh (121), 919 (27)
	DMF	N_2S_2, N'_3S_2L	516 (359), 621sh (122), 926 (31)
$[Ni_2(\mathbf{9})L]^{2+}$ (**12**)	CH_3CN	N_2S_2, N'_3S_2L	516 (356), 615sh (121), 916 (38)
	CH_2Cl_2	N_2S_2, N'_3S_2L	511 (590), 634sh (151), 948 (39)
$[Ni_2(\mathbf{9})(NCS)]^{1+}$ (**13**)	DMF	$2 \times N_3S_3$	513 (472), 621sh (139), 950 (39)
and their oxidized derivatives			
$[Ni^{III}Ni^{II}(\mathbf{1})_3]^{2+}$ $(\mathbf{3})^{2+}$	DMF	$2 \times N_3S_3$	473 (6753), 580 (4022)
$[Ni_2(\mathbf{1})_2]^{3+}$ $(\mathbf{2})^{3+}$	MeOH	$2 \times N_2S_2$	476 (1865), 626 (1242), 972 (1242)
$[Ni_2(\mathbf{4})]^{3+}$ $(\mathbf{5})^{3+}$	MeOH	$2 \times N_2S_2$	458 (2060), 581 (1034), 936 (376)
$[Ni_2(\mathbf{9})L]^{3+}$ $(\mathbf{10})^{3+}$	MeOH	N_2S_2, N'_3S_2L	462 (690), 584 (839), 898 (279)

[a] N and N′ denote primary and secondary nitrogen atoms.

plexes **11** and **13** in the solid-state. This is strongly supported by their electronic absorption spectral data. UV/Vis spectral data for all complexes are summarized in Table 2.

The spectra recorded for complexes **10**, **12**, and **13** are very similar − even in solvents of different donor strength. The spectrum of **10** in MeOH solution is representative of all the compounds, with an intense absorption at λ_{max} = 516 nm, a shoulder at 621 nm, and a weak absorption at 926 nm. It is noted that the position of the weak absorption in the 920 to 950 nm region appears to be dependent on the choice of the solvent.

The comparisons of the present UV/Vis spectral data with those of four-coordinate NiN_2S_2 complexes (**2**) or those of octahedral NiN_3S_3 complexes (**3**), respectively, clearly reveal the spectra of **10**−**13** to be due to superpositions of the electronic transitions of planar NiN_2S_2 and octahedral NiN_3S_2L chromophores. The intense band in the narrow range 506 to 516 nm, for example, is readily assigned to an electronic transition of a planar NiN_2S_2 unit. These bands are of approximately half the intensity of the corresponding band at 503 nm in **2**, which is consistent with the presence of only one such unit in complexes **10**−**13**. The other two bands at ca. 620 and ca. 930 to 950 nm are characteristic for an octahedral NiN_3S_2L complex.[12][20] Complex **3**, with two octahedral NiN_3S_3 units, exhibits absorptions at similar positions at 593 ($^3A_{2g}\rightarrow{}^3T_{1g}$) and 922 nm ($^3A_{2g}\rightarrow{}^3T_{2g}$), both of which again exhibit approximately twice the intensity of the respective bands of compounds **10**−**13**. This again supports the presence of only one NiN_3S_2L chromophore per dinuclear complex, as is required for complexes composed of one NiN_2S_2 and one NiN_3S_2L chromophore. The solvent dependence of the ($^3A_{2g}\rightarrow{}^3T_{2g}$) transitions around 920−950 nm is taken as an indication for the presence of an exchangeable solvent molecule in the coordination sphere of the octahedral NiN'_3S_2L fragment.

Electrochemistry

Complexes **10**, **13**, and **5** (for comparative purposes) were further characterized by cyclic voltammetry. The electrochemical properties of complex **2** have been reported previously.[12] Cyclic voltammograms (CV′s) were recorded in CH_3CN solution (for **5** and **10**) or DMF solution (for **13**) with tetra-*n*-butylammonium hexafluorophosphate as the supporting electrolyte and ferrocene as internal standard. In the following discussion, all redox potentials are referenced versus SCE.[21] Table 3 summarizes the measured potentials.

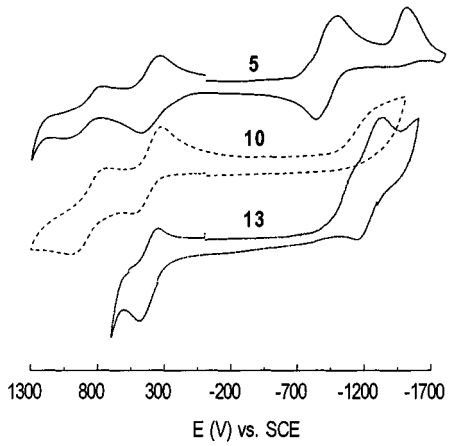

Figure 4. Cyclic voltammograms of complexes **5** and **10** in CH_3CN solution and of **13** in DMF solution at 295 K. Experimental conditions: [**5**], [**10**], [**13**] ca. $1\cdot10^{-3}$ M, Pt disk working electrode, Ag wire reference electrode, 0.1 M [nBu$_4$N][PF$_6$], scan rate 200 $mV\cdot s^{-1}$

The CV of complex **10** in acetonitrile solution is shown in Figure 4. Figure 4 shows, in the anodic potential region, two oxidation waves at $E^1_{1/2}$ = +0.88 V and at $E^2_{1/2}$ = +0.41 V vs SCE − an irreversible reduction wave occurred at ≈ −1.1 V. The electrochemical behavior of complexes **2**

Table 3. Electrochemical data (E/V) for dinuclear nickel-amine-thiolate complexes[a]

complex	donor set(s)[b]	$E^1_{1/2}$	$E^2_{1/2}$	$E^3_{1/2}$	$E^4_{1/2}$
$[Ni_2(\mathbf{1})_2]^{2+}$ (**2**)[c,d]	$2 \times N_2S_2$	+0.89 (irr)	+0.44 (79)	−0.86 (79)	−1.49 (irr)
$[Ni_2(\mathbf{4})]^{2+}$ (**5**)[c]	N_2S_2, N'_2S_2	+0.91 (265)	+0.42 (133)	−0.91 (142)	−1.51 (irr)
$[Ni_2(L^1)][ClO_4]_2$[e]	$2 \times N'_2S_2$	+1.35 (qr)	0.94 (r)	−0.93 (r)	−1.61 (qr)
$[Ni_2(\mathbf{9})(L)]^{2+}$ (**10**)[c]	N_2S_2, N'_3S_2L	+0.88 (251)	+0.41 (159)	n.o.	n.o.
$[Ni_2(\mathbf{9})(NCS)]^{+}$ (**13**)[f]	N_2S_2, N'_3S_2L	n.o.	+0.42 (137)	−1.23 (183)	n.o.
$[Ni_2(\mathbf{1})_3]^{2+}$	$2 \times N_3S_3$	+0.46 (84)	−0.02 (73)		

[a] Solutions of complexes were ca. $1 \cdot 10^{-1}$ M in supporting electrolyte (nBu$_4$NPF$_6$) and ca. $1 \cdot 10^{-3}$ M in sample; Pt disk working electrode, Ag wire reference electrode, scan rate 200 mV s^{-1}, $E^{\times}_{1/2} = (E^{ox}_p + E^{red}_p)/2$ for reversible one-electron transfer processes; oxidation (E^{ox}_p) or reduction peak potentials (E^{red}_p) are given for irreversible (irr) processes; number in parentheses denote peak-to-peak separations $\Delta E_p = |E^{ox}_p - E^{red}_p|$, n.o. = not observed. − [b] N and N′ denote primary and secondary nitrogen atoms. − [c] Solvent = acetonitrile. − [d] Values taken from ref.[12] − [e] L^1 = macrocyclic N_4S_2 ligand,[9] reported potentials were converted into the SCE [E (V) vs SCE = E (V) vs Ag/Ag$^+$ + 0.38 V] according to Table 1 in ref.[21], peak-to-peak separations were reported as reversible (r) or quasi-reversible (qr). − [f] Solvent = *N*,*N*-dimethylformamide.

and **5** in the anodic potential region is very similar, with two well-separated oxidation waves at $E^1_{1/2} \approx +0.90$ V and at $E^2_{1/2} \approx +0.41$ V vs SCE (see Table 3). In the following, we will discuss only processes that occur in the anodic potential region.[22]

The oxidation waves at $E^1_{1/2}$ and at $E^2_{1/2}$ of all complexes exhibit very large peak-to-peak separations, indicating that the corresponding charge-transfer processes are electrochemically not reversible. Is was not possible by controlled-potential coulometry to determine the number of electrons transferred during these processes, since at ambient temperature the oxidized species of complexes **2**, **5**, and **10** are not stable on the timescale of a coulometric experiment. Electrolysis of complex **10** at an applied potential of +0.60 V vs SCE, for example, resulted in a color change from red to transient dark-green. These transient dark-green solutions were also obtained by chemical oxidation of the complexes. Figure 5 shows the UV/Vis spectra taken for complex **10** before and after its oxidation. The observed spectral changes clearly show the oxidized species to be thermally unstable at room temperature. The fate of the oxidized species is discussed below. For now we estimate the half-life $\tau_{1/2}$ of the oxidized species to be ca. 15 min (from the decrease in ε_M at 584 nm with time). Complexes **2** and **5** behaved similarly, producing transient dark-green solutions upon electrolysis or chemical oxidation.

In a similar way to transition metal phenolato complexes, the oxidation of a transition metal thiophenolato complex can, in principle, be either metal- or ligand-centered.[23] There are several points that imply that the processes at $E^2_{1/2}$ and $E^1_{1/2}$ involve metal-centered one-electron transfer reactions subsequently producing mixed-valent $Ni^{III,II}$ and $Ni^{III,III}$ species, respectively. First of all, it is well-known that thiolate ligands are powerful in stabilizing Ni in the trivalent state.[24] Secondly, the number of observed oxidation waves (N) and their separations ($\Delta E = |E^1_{1/2} - E^2_{1/2}|$) are invariably $N = 2$ and $\Delta E \approx 0.45$ V, respectively, for all complexes. N matches with the number of metal atoms per complex and the value of 0.45 V for ΔE would be consistent with the presence of a mixed-valent $Ni^{III}Ni^{II}$ complex that is very stable to disproportionation ($K_{disp.} \approx 10^{-7}$), respectively. Thirdly, the UV/Vis spectra of all the transient dark-green solutions exhibit three very strong absorptions at around 470, 600, and 900 nm, which are characteristic of trivalent NiN_xS_y complexes.[12][20] Since the spectra of the oxidized species lack any characteristic absorptions for a planar NiN_2S_2 chromophore, it is assumed that the oxidations are accompanied by changes in the coordination environment of the planar NiN_2S_2 site. The broad peak-to-peak separations noted earlier would be consistent with this view.

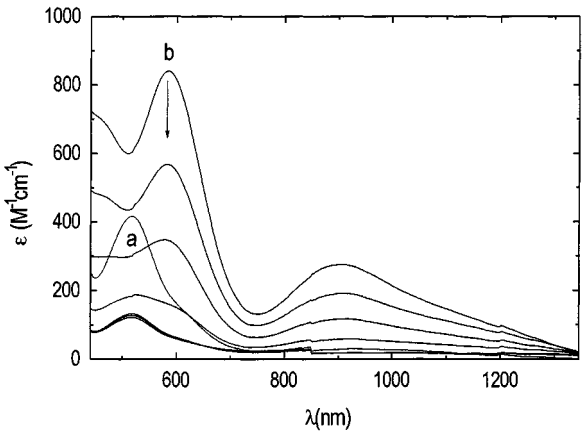

Figure 5. Oxidation of complex **10** with bromine in MeOH followed by UV/Vis spectroscopy (a: spectrum before, b: spectrum after addition of bromine). The other spectra were taken at 6 min intervals (the arrow indicates the evolution of the spectra with time)

A metal-centered nature for these oxidations is also supported by X-band EPR spectroscopic studies of frozen (77 K) solutions. Figure 6 shows the EPR spectrum of the green solution prepared by chemical oxidation of **10**. It reveals an axial signal as the main component with estimated g values of $g_\perp \approx 4.7$ and $g_\parallel \approx 2.1$, which are indicative of an $S = {}^3/_2$ spin ground state.[25] Hyperfine splitting due to ligand nitrogens could not be observed. Similar $S = {}^3/_2$ signals were previously observed for $\mathbf{3}^{2+}$ and for other mixed-valent $Ni^{III}Ni^{II}$ amine-thiolate complexes.[12] The $S = {}^3/_2$ ground states of these complexes are attained by an intramolecular ferromagnetic exchange interaction between low-spin Ni^{III} ($S = {}^1/_2$) and Ni^{II} ($S = 1$) ions. However, in the absence of more detailed spectroscopic data one can only

speculate about the electronic structure of the oxidized species.

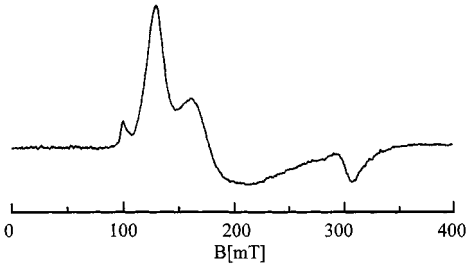

Figure 6. Frozen solution (77 K) X-band EPR spectrum of $\mathbf{10}^{+}$. Conditions: microwave frequency: ν = 9.02 GHz; microwave power: 2 mW; modulation frequency: 100 kHz; modulation amplitude: 10 gauss

The observation of an oxidation wave at $E^{2}_{1/2}$ = +0.42 V vs SCE for the isothiocyanate complex **13** in DMF solution also deserves some comment. Although the thiocyanate ion itself is redoxactive,[26] its oxidation can be ruled out since $E_{1/2}$ for this process is at +0.77 V vs SCE.[27] It is thus likely that this oxidation also corresponds to a metal-centered oxidation forming a Ni^{III} species. It was not possible to prepare the oxidized species by chemical or electrochemical oxidation, presumably due to its very rapid decomposition.

Chemical Oxidation of Metal Complexes

Complexes **2**, **5**, and **10** could also be chemically oxidized. Whereas addition of iodine to methanolic solutions of the complexes had no effect, treatment with bromine resulted in a sudden color change from red to dark-green. It was necessary to use less than 0.2 equiv. of oxidant to observe the transient green color. Figure 7 shows the UV/Vis spectral changes that occurred upon addition of ca. 0.1 equivalent of oxidant to a solution of complex **2** in methanol. The spectrum recorded directly after sample preparation is identical to that taken for a sample prepared by electrochemical oxidation, indicating that both methods produce the same species. In a similar way to **10** the oxidation product of complex **2** is thermally unstable.

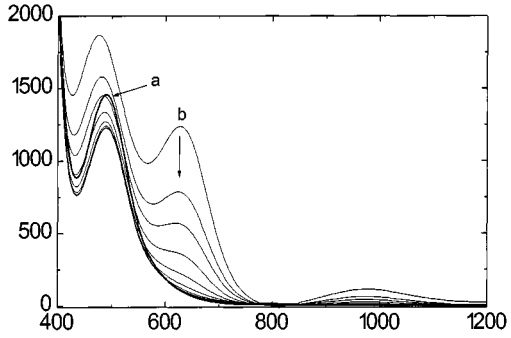

Figure 7. Oxidation of complex **2** with bromine in MeOH followed by UV/Vis spectroscopy (a: spectrum before, b: spectrum after addition of bromine). The other spectra were taken at 6 min intervals (the arrow indicates the evolution of the spectra with time)

The oxidized species of all complexes were allowed to decompose at ambient temperature. In the case of complexes **5** and **10** the resulting pale-green reaction mixtures contained a variety of new products that could not be separated. For complex **2**, however, oxidation resulted in the formation of the benzisothiazole derivative **14**[28] in high yield. The same compound is also obtained by treatment of the ligand, $H_1\mathbf{1} \cdot 2$ HCl, with iodine in methanol in the presence of base. It should be noted that the complexes could not be oxidized with iodine and this is taken as another indication that the oxidations are primarily metal-centered with the formation of intermediate Ni^{III} species.

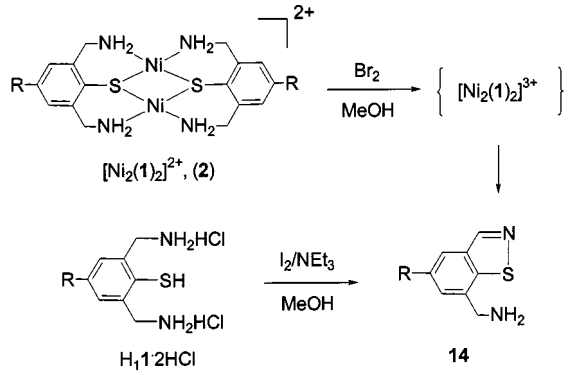

Scheme 5. Oxidation of $H_1\mathbf{1} \cdot 2$ HCl and $[Ni_2(\mathbf{1})_2][ClO_4]_2$ (**2**)

Conclusion

The aim of controlling the reactivity of dinuclear nickel amine-thiolate complexes such as **5** has been achieved by a slight ligand modification. The constituent amine-thiophenolate units in $H_2\mathbf{9}$ retain their typical coordination mode but the additional NH donor blocks one of the two potentially free coordination sites found for **5**. The position *trans* to this donor is the reactive site of the present complexes. Solvent molecules and pseudo-halide ions bind to this site; the coordination of a halide ion has been observed for the first time. The latter substituent may be substituted by other co-ligands such as H^{-} or CN^{-}, and the influence of such substituents on the $Ni^{III,II}$ redox-potentials could be studied. These studies could also be of importance in attempts to model structural and functional features of dithiolate-bridged $[M(\mu\text{-}SR)_2M]$ structures found in metalloproteins, as for instance in [NiFe] hydrogenase from *Desulfovibrio gigas*.

Experimental Section

Materials and Methods: Compounds **7**,[13] $H_1\mathbf{1} \cdot 2$ HCl,[10] $[Ni_2(\mathbf{1})_2][ClO_4]_2$,[12] and $[Ni_2(\mathbf{4})][ClO_4]_2$[13] were prepared as previously described. All other chemicals were of reagent grade and used without further purification. Solvents were predried over molecular sieves and freshly distilled from appropriate drying agents. – ^{1}H-NMR and $^{13}C\{^{1}H\}$-NMR spectra were recorded on a Bruker AVANCE DPX 200 spectrometer. All chemical shifts are quoted on the δ scale with TMS or the solvent as internal standard. Coupling

constants are expressed in Hz. − Melting points were determined in capillaries and are uncorrected. − CHN-Analyses were determined with a Perkin−Elmer Elemental Analyzer 240. − IR spectra were recorded on a Bruker VECTOR 22 FT-IR-spectrophotometer as KBr pellets. − Absorption spectra were recorded on a Jasco V-570 UV/VIS/NIR spectrometer. − Room temperature magnetic susceptibility measurements were carried out with a Johnson Matthey model Mark II magnetic susceptibility balance. Experimental susceptibility data were corrected for the underlying diamagnetism using Pascal's constants.[29] − Cyclic voltammetry measurements were carried out at 25°C with an EG&G Princeton Applied Research Potentiostat/Galvanostat Model 263 A. The cell contained a Pt working electrode, a Pt wire auxiliary electrode, and an Ag wire as a reference electrode. Concentration of solutions were 0.1 M in supporting electrolyte ($Bu^n_4NPF_6$) and ca. 1×10^{-3} M in sample. Ferrocenium/ferrocene was used as the internal standard. All potentials were converted into the SCE reference [E (V) vs SCE = E (V) vs Fc^+/Fc − 0.38 V in CH_3CN].[21] EPR spectra were recorded using a conventional Varian X-band spectrometer with 100 kHz modulation.

***N*,*N*′-Bis[2-*tert*-butylsulfanyl-3-hydroximinomethyl-5-*tert*-butylbenzylidene]diethylenetriamine (8):** To a stirred solution of aldehyde **7** (587 mg, 2.00 mmol) in absolute ethanol (10 mL) was added a solution of *N*,*N*-bis(2-aminoethyl)amine (103 mg, 1.00 mmol) in ethanol (10 mL). After stirring for 2 h at 60°C, a solution of $NaBH_4$ (200 mg, 5.27 mmol) in ethanol (20 mL) was added, and the resulting homogeneous reaction mixture was stirred for further 12 h. Water (50 mL) was then added and the pH of the solution was adjusted to 1 by the addition of hydrochloric acid to destroy excess reducing equivalents. The mixture was stirred for an additional 30 min, the solution was made alkaline (final pH ≈ 12−13) by addition of 5 M KOH solution, and then extracted with dichloromethane (3 × 50 mL). The combined extracts were dried with $MgSO_4$, filtered, and the filtrate evaporated to dryness under reduced pressure. The pale-yellow residue was purified by column chromatography (SiO_2) using 10% MeOH in CH_2Cl_2 as eluent. Yield 521 mg (79%), m.p. 154°C. − ^{1}H NMR (5% CD_3OD/$CDCl_3$): δ = 8.88 (s, 2 H, ArC*H*), 7.79 (d, $^4J_{H,H}$ = 2.0 Hz, 2 H, Ar*H*), 7.43 (d, $^4J_{H,H}$ = 2.0 Hz, 2 H, Ar*H*), 4.00 (s br, 4 H, ArCH_2), 2.60 (s, 8 H, CH_2), 1.27 (s, 18 H, CH_3), 1.18 (s, 18 H, CH_3). − ^{13}C NMR (CD_3OD): δ = 153.8, 151.9, 147.0, 140.1, 130.2, 129.5, 123.6, 53.7, 50.4, 49.0, 47.3, 35.9, 31.9, 31.8.

***N*,*N*′-Bis[3-aminomethyl-5-*tert*-butyl-2-thiobenzyl]diethylenetriamine Pentahydrochloride ($H_2$9 · 5 HCl):** To a solution of **8** (658 mg, 1.00 mmol) in liquid ammonia (50 mL) was added sodium in small portions at −70°C, until the blue color of the reaction mixture persisted for at least 1 h (without adding further reducing equivalents). After stirring for an additional 1 h, excess sodium was destroyed by addition of solid ammonium chloride, and the solvent was evaporated at atmospheric pressure. The resulting solid was hydrolyzed with methanol (30 mL) followed by 6 M hydrochloric acid (final pH ≈ 1), and then evaporated to dryness under reduced pressure. For purification, the remaining solid was dissolved in ethanol (50 mL), filtered to remove NaCl and NH_4Cl, and evaporated to dryness. This procedure was repeated two more times. The resulting solid was sufficiently pure for metal complex syntheses. Yield 476 mg (68%). − IR (KBr): $\tilde{\nu}$ = 3417 cm^{-1} br (NH), 2400 sh (SH). − ^{1}H NMR (D_2O): δ = 7.79 (s, 4 H, Ar*H*), 4.66 (s, 4 H, ArCH_2), 4.50 (s, 4 H, ArCH_2), 3.70 (s, 8 H, CH_2), 1.39 (s, 18 H, CH_3). − ^{13}C NMR (D_2O): δ = 153.2, 136.7, 134.2, 130.1, 129.8, 127.3, 51.4, 44.0, 43.3, 42.9, 34.6, 30.7.

[Ni_2(9)(L)][ClO_4]$_2$ (10, L = H_2O): ***CAUTION!*** *Transition metal perchlorates are hazardous and may explode. Only small quantities should be prepared and great care taken.* To a solution of H_2**9** · 5 HCl (0.700 g, 1.00 mmol) and $Ni(ClO_4)_2 \cdot 6\,H_2O$ (731 mg, 2.00 mmol) in methanol (10 mL) was added a solution of NEt_3 (0.505 g, 0.500 mmol) in MeOH (1 mL). The reaction mixture was stirred for 5 min at 60°C, during which time a red crystalline precipitate formed. The solid was filtered off, washed with cold MeOH (2 × 1 mL) and ether, and dried in air. Yield: 487 mg (57%). − $C_{28}H_{45}Ni_2N_5S_2(ClO_4)_2H_2O$ (850.12): calcd. C 39.56, H 5.57, N 8.24; found C 39.64, H 5.42, N 8.18. − IR (KBr): $\tilde{\nu}$ = 3424 cm^{-1} br (OH), 3288, 3244, 3184, 3162, (NH + NH_2), 1150 s, 1115 s, 1089 vs (ClO_4^-).

[Ni_2(9)Cl][Cl] · 2 CH_3CN · H_2O (11): To a solution of H_2**9** · 5 HCl (0.700 g, 1.00 mmol) and $NiCl_2 \cdot 6\,H_2O$ (475 mg, 2.00 mmol) in acetonitrile (10 mL) was added a solution of NEt_3 (0.505 g, 0.500 mmol) in acetonitrile (1 mL). The reaction mixture was stirred for 5 min at 60°C, during which time a red crystalline precipitate formed. The solid was filtered off, washed with cold acetonitrile (2 × 1 mL) and ether, and dried in air. The crude product was recrystallized once from MeOH/CH_3CN. Yield: 530 mg (66%). − $C_{28}H_{45}Ni_2N_5S_2Cl_2(H_2O)(CH_3CN)_2$ (804.25): calcd. C 47.79, H 6.64, N 12.19; found C 47.43, H 6.42, N 11.87.

[Ni_2(9)(L)][BPh_4]$_2$ (12, L= H_2O): To a solution of complex **10** (86 mg, 0.10 mmol) in MeOH (10 mL) was added a solution of $NaBPh_4$ (50 mg, 0.15 mmol) in MeOH (1 mL). The solution was stirred for 20 min at room temperature, during which time a red crystalline precipitate formed. The solid was filtered off, washed with cold MeOH (2 × 1 mL) and dried in air. Yield: 106 mg (82%). − $C_{28}H_{45}Ni_2N_5S_2(BPh_4)_2H_2O$ (1289.68): calcd. C 70.78, H 6.80, N 5.43; found C 70.98, H 6.73, N 5.18. − IR (KBr): $\tilde{\nu}$ = 735 cm^{-1} s, 707 s (BPh_4^-).

[Ni_2(9)(NCS)][OH·H_2O] (13): To a solution of **10** (33 mg, 40 μmol) in MeOH (5 mL) was added a solution of NH_4SCN (4.6 mg, 60 μmol) in MeOH (2 mL). The resulting red solution was stirred for 1 h, during which time a dark-red microcrystalline solid precipitated. The solid was filtered off, washed with 2 mL of MeOH, and dried in air. Yield: 24 mg (83%), m.p. 344−346°C (decomp.). − IR (KBr): $\tilde{\nu}$ = 2090 cm^{-1} vs (NCS^-). − $C_{29}H_{48}Ni_2N_6S_3O_2$ (726.33): calcd. C 47.96, H 6.66, N 11.57; found C 47.83, H 6.43, N 11.18.

Oxidation of $H_1$1 · 2 HCl **(Preparation of 7-Aminomethyl-5-*tert*-butylbenzisothiazol) (14):** To a solution of H_1**1** · 2 HCl (297 mg, 1.00 mmol) and NEt_3 (556 mg, 5.50 mmol) in methanol (30 mL) was added a solution of iodine (508 mg, 2.00 mmol) in methanol (20 mL), and the reaction mixture was stirred for 2 h. The organic solvent was removed under reduced pressure, 20 mL of 1 M NaOH solution was added to the residue, and the product extracted with dichloromethane (3 × 50 mL). The combined extracts were dried with K_2CO_3, filtered, and evaporated to dryness to give 198 mg (89%) of **14** as a pale yellow solid. The crude product was purified by column chromatography using 10% MeOH in CH_2Cl_2 as eluent. M.p. 242−245°C. − ^{1}H NMR (CD_3OD/2% DCl): δ = 9.06 (s, 1 H, C*H*=N), 8.29 (d, ^4J = 1.6 Hz, 1 H, Ar*H*), 7.92 (d, ^4J = 1.6 Hz, 1 H, Ar*H*), 4.47 (s, 2 H, CH_2), 1.50 (s, 9 H, CH_3). − ^{13}C NMR (CD_3OD): δ = 158.0, 152.0, 150.5, 139.4, 128.8, 126.5, 122.7, 43.7, 36.4, 32.2.

Oxidation of [Ni_2(1)$_2$][ClO_4]$_2$: To a solution of complex [Ni_2(**1**)$_2$][ClO_4]$_2$ (200 mg, 0.262 mmol) and NEt_3 (303 mg, 0.3 mmol) in methanol (40 mL) was added a freshly prepared solution of bromine (34.2 mg, 0.214 mmol) in methanol (2 mL) at room temperature. The resulting transient dark-green solution was stirred for 30 min, during which time the color of the solution changed to dark-red. This process was repeated three more times to give a pale-green solution. The organic solvent was removed under reduced

pressure, 20 mL of 1 M NaOH solution (20 mL) was added to the residue, and the product extracted with dichloromethane (3 × 50 mL). The combined extracts were dried with K_2CO_3, filtered, and evaporated to dryness. The pale-green residue was dissolved in 2 mL of ethanol and acidified with 3 drops of 12 M HCl. Addition of ether caused precipitation of an off-white solid, which was filtered off and dried in air. Yield: 84 mg (73%). The analytical data are identical with those of compound **14**.

Crystal Structure Determination: Single crystals of complexes **11** and **13** suitable for X-ray structure analysis could be obtained by slow evaporation of acetonitrile/methanol solutions of the complexes. The crystals were mounted on glass fibers using perfluoropolyether oil. Crystal data were collected at 180(2) K, using a Bruker SMART CCD diffractometer. Graphite monochromated Mo-*K*α radiation (0.71073 Å) was used throughout. The data were processed with SAINT[30] and corrected for absorption using SADABS (transmission factors: 1.00−0.11 for **11**, 1.00−0.77 for **13**).[31]

Crystal data and refinement details for **11** ($C_{32}H_{53}Cl_2N_7Ni_2OS_2$, *M*r = 804.25): crystal size 0.52 × 0.46 × 0.32 mm, monoclinic, space group *P*2(1)/c, *a* = 14.251(3) Å, *b* = 21.351(4) Å, *c* = 12.805(3) Å, β = 94.28(3)°, *V* = 3885(1) Å^3, *Z* = 4, μ(Mo-*K*α) = 1.25 mm^{-1}, D_c = 1.375 g·cm^{-3}, *F*(000) = 1696, 24550 reflections measured, 9179 unique (R_{int} 0.1545), 5320 observed reflections [$I > 2\sigma(I)$]. The structure was solved by direct methods using the program SHELXS-86[32] and refined by full-matrix least-squares techniques against F^2 using SHELXL-93.[33] Positional and anisotropic atomic displacement parameters were refined for all nonhydrogen atoms, except for the C and N atoms of two acetonitrile molecules (refined isotropically). Hydrogen atoms were placed geometrically and positional parameters were refined using a riding model. Isotropic atomic displacement parameters for hydrogen atoms were constrained to be 1.2 (1.5 for methyl groups). Final residuals *R*1 = 0.0780, *wR*2 = 0.1846 [$I > 2\sigma(I)$], *R*1 = 0.1236, *wR*2 = 0.2126 (all data), largest difference peak, $\Delta\rho_{max}$ = 1.567 eÅ^{-3}, and hole $\Delta\rho_{min}$ = −1.265 eÅ^{-3}.

Crystal data and refinement details for **13** ($C_{29}H_{48}Ni_2N_6S_3O_2$, *M*r = 726.33): crystal size 0.75 × 0.51 × 0.16 mm, monoclinic, space group *C*c (no. 9), *a* = 11.204(2) Å, *b* = 25.651(5) Å, *c* = 12.187(2) Å, β = 98.68(3)°, *V* = 3462(1) Å^3, *Z* = 4, μ(Mo-*K*α) = 1.303 mm^{-1}, D_c = 1.393 g·cm^{-3}, *F*(000) = 1536, 12152 reflections measured, 4998 unique (R_{int} 0.0261), 4912 observed reflections [$I > 2\sigma(I)$]. The structure was solved by direct methods using the program SHELXS-86[32] and refined by full-matrix least-squares techniques against F^2 using SHELXL-93.[33] Positional and anisotropic atomic displacement parameters were refined for all non-hydrogen atoms, except for the oxygen atoms of a water molecule and a hydroxide ion (refined isotropically). Hydrogen atoms were placed geometrically and positional parameters were refined using a riding model. The OH^- and H_2O hydrogen atoms were located unambiguously from difference Fourier maps. Isotropic atomic displacement parameters for hydrogen atoms were constrained to be 1.2 (1.5 for methyl groups). The Flack *X* parameter (absolute structure parameter) was calculated to be 0.03(2) for the present structure and 0.98(2) for the inverted structure, thus providing strong evidence that the absolute structure has been assigned correctly.[34] Final residuals *R*1 = 0.0388, *wR*2 = 0.1148 [$I > 2\sigma(I)$], *R*1 = 0.0406, *wR*2 = 0.1185 (all data), largest difference peak, $\Delta\rho_{max}$ = 0.518 eÅ^{-3}, and hole $\Delta\rho_{min}$ = −0.501 eÅ^{-3}.

Crystallographic data (excluding structure factors) for the structures reported in this paper have been deposited with the Cambridge Crystallographic Data Centre as supplementary publication no. CCDC-132820 (**11**) and CCDC-121428 (**13**). Copies of the data can be obtained free of charge on application to CCDC, 12 Union Road, Cambridge CB2 1EZ, UK [Fax: +44(1223) 336-033; E-mail: deposit@cam.ac.uk].

Acknowledgments

This work was supported by the Deutsche Forschungsgemeinschaft. The author thanks Prof. Dr. H. Vahrenkamp for his generous support. Financial support from the Wissenschaftliche Gesellschaft Freiburg and the Graduiertenkolleg "Ungepaarte Elektronen" is also gratefully acknowledged. Prof. D. Siebert and G. Steinfeld are thanked for recording EPR spectra.

[1] [1a] J. G. Hughes, R. Robson, *Inorg. Chim. Acta.* **1979**, *35*, 87−92. − [1b] M. Louey, P. D. Nichols, R. Robson, *Inorg. Chim. Acta.* **1980**, *47*, 87−96. − [1c] P. Iliopoulos, K. S. Murray, R. Robson, J. Wilson, G. A. Williams, *J. Chem. Soc., Dalton Trans.* **1987**, 1585−1591. − [1d] A. M. Bond, M. Haga, I. S. Creece, R. Robson, J. C. Wilson, *Inorg. Chem.* **1989**, *28*, 559−566. − [1e] B. F. Hoskins, C. J. McKenzie, R. Robson, L. Zhenrong, *J. Chem. Soc., Dalton Trans.* **1990**, 2637−2641. − [1f] B. F. Hoskins, R. Robson, G. A. Williams, J. C. Wilson, *Inorg. Chem.* **1991**, *30*, 4160−4166.

[2] [2a] B. Krebs, G. Henkel, *Angew. Chem.* **1991**, *103*, 785−804; *Angew. Chem. Int. Ed. Engl.* **1991**, *30*, 769−788. − [2b] I. G. Dance, *Polyhedron* **1986**, *5*, 1037−1104. − [2c] P. J. Blower, J. R. Dilworth, *Coord. Chem. Rev.* **1987**, *76*, 121−185.

[3] [3a] A. J. Atkins, A. J. Blake, M. Schröder, *J. Chem. Soc., Chem. Commun.* **1993**, 1662−1665. − [3b] A. J. Atkins, D. Black, A. J. Blake, A. Marin-Becerra, S. Parsons, L. Ruiz-Ramirez, M. Schröder, *J. Chem. Soc., Chem. Commun.* **1996**, 457−464. − [3c] N. D. J. Branscombe, A. J. Blake, A. Marin-Becerra, W.-S. Li, S. Parsons, L. Ruiz-Ramirez, M. Schröder, *J. Chem. Soc., Chem. Commun.* **1996**, 2573−2574.

[4] [4a] S. Brooker, P. D. Croucher, *J. Chem. Soc., Chem. Commun.* **1995**, 1493−1494. − [4b] S. Brooker, P. D. Croucher, *J. Chem. Soc., Chem. Commun.* **1995**, 2075−2076. − [4c] S. Brooker, P. D. Croucher, F. M. Roxburgh, *J. Chem. Soc., Dalton Trans.* **1996**, 3031−3037. − [4d] S. Brooker, P. D. Croucher, *J. Chem. Soc., Chem. Commun.* **1997**, 459−460.

[5] P. E Kruger, V. McKee, *J. Chem. Soc., Chem. Commun.* **1997**, 1341−1342.

[6] For biological, dithiolate-bridged Cu/Cu systems, see: [6a] T. Tsukihara, H. Aoyama, E. Yamashita, T. Tomizaki, H. Yamaguchi, K. Shinzawa-Itoh, R. Nakashima, R. Yaono, S. Yoshikawa, *Science* **1995**, *269*, 1069−1074. − [6b] S. Iwata, C. Ostermeier, B. Ludwig, H. Michel, *Nature* **1995**, *376*, 660−669.

[7] For biological, dithiolate-bridged Fe/Ni systems, see: [7a] A. Volbeda, M.-H. Charon, C. Piras, E. C. Hatchikian, M. Frey, J. C. Fontecilla-Camps, *Nature* **1995**, *373*, 580−587. − [7b] A. Volbeda, E. Garcin, C. Piras, A. L. de Lacey, V. M. Fernandez, E. C. Hatchikian, M. Frey, J. C. Fontecilla-Camps, *J. Am. Chem. Soc.* **1996**, *118*, 12989−12996. − [7c] M. A. Halcrow, *Angew. Chem.* **1995**, *107*, 1307−1310; *Angew. Chem. Int. Ed. Engl.* **1995**, *34*, 1193−1197.

[8] For biological dithiolate-bridged Fe/Fe systems, see: J. W. Peters, W. N. Lanzilotta, B. J. Lemon, L. C. Seefeldt, *Science* **1998**, *282*, 1853−1858.

[9] S. Brooker, P. D. Croucher, T. C. Davidson, G. S. Dunbar, A. J. McQuillan, G. B. Jameson, *J. Chem. Soc., Chem. Commun.* **1998**, 2131−2132.

[10] B. Kersting, *Eur. J. Inorg. Chem.* **1998**, 1071−1077.

[11] E. C. Constable, *Metals and Ligand Reactivity*, VCH, Weinheim, **1996**.

[12] [12a] B. Kersting, D. Siebert, *Inorg. Chem.* **1998**, *37*, 3820−3828. − [12b] B. Kersting, D. Siebert, *Eur. J. Inorg. Chem.* **1999**, 189−193.

[13] B. Kersting, G. Steinfeld, J. Hausmann, *Eur. J. Inorg. Chem.* **1999**, 179−187.

[14] [14a] D. Sellmann, J. Utz, F. W. Heinemann, *Eur. J. Inorg. Chem.* **1999**, 341−348. − [14b] D. Sellmann, J. Utz, F. W. Heinemann, *Inorg. Chem.* **1999**, *38*, 459−466. − [14c] D. Sellmann, W. Sog-

lowek, F. Knoch, M. Moll, *Angew. Chem.* **1989**, *101*, 1244−1245; *Angew. Chem. Int. Ed. Engl.* **1989**, *28*, 1271−1272. − [14d] D. Sellmann, W. Soglowek, M. Moll, *Z. Naturforsch.* **1992**, *47b*, 1105−1114.
[15] K. Nakamoto, *Infrared and Raman Spectra of Inorganic and Coordination Compounds*, Wiley, New York, **1978**.
[16] [16a] G. Musie, P. J. Farmer, T. Tuntulani, J. H. Reibenspies, M. Y. Darensbourg, *Inorg. Chem.* **1996**, *35*, 2176−2183. − [16b] G. A. Lawrance, M. Maeder, T. M. Manning, M. A. O′Leary, B. W. Skelton, A. H. White, *J. Chem. Soc., Dalton Trans.* **1990**, 2491−2495.
[17] K. Osakada, T. Yamamoto, A. Yamamoto, A. Takenaka, Y. Sasada, *Acta Crystallogr.* **1984**, *C40*, 85−87.
[18] P. E. Riley, K. Seff, *Inorg. Chem.* **1972**, *11*, 2993−2999.
[19] F. A. Cotton, G. Wilkinson, *Advanced Inorganic Chemistry*, 5th ed., John-Wiley & Sons, New York, **1988**.
[20] H.-J. Krüger, R. H. Holm, *J. Am. Chem. Soc.* **1990**, *112*, 2955−2963.
[21] N. G. Connelly, W. E. Geiger, *Chem. Rev.* **1996**, *96*, 877−910.
[22] The processes that occur at $E < 0$ V will be discussed in more detail in a subsequent paper. G. Steinfeld, B. Kersting, unpublished results.
[23] B. Adam, E. Bill, E. Bothe, B. Goerdt, G. Haselhorst, K. Hildenbrand, A. Sokolowski, S. Steenken, T. Weyhermüller, K. Wieghardt, *Chem. Eur. J.* **1997**, *3*, 308−319.
[24] [24a] H.-J. Krüger, R. H. Holm, *Inorg. Chem.* **1987**, *26*, 3645−3647. − [24b] T. Krüger, B. Krebs, G. Henkel, *Angew. Chem.* **1992**, *104*, 71−72; *Angew. Chem. Int. Ed. Engl.* **1992**, *31*, 54−56. − [24c] J. D. Franolic, W. Y. Wang, M. Millar, *J. Am. Chem. Soc.* **1992**, *114*, 6587−6588. − [24d] D. Sellmann, W. Prechtel, F. Knoch, M. Moll, *Z. Naturforsch.* **1992**, *47b*, 1411−1423. − [24e] J. Hanss, H.-J. Krüger, *Angew. Chem.* **1998**, *110*, 366−369; *Angew. Chem. Int. Ed. Engl.* **1998**, *37*, 360−363. − [24f] T. Beissel, F. Birkelbach, E. Bill, T. Glaser, F. Kesting, C. Krebs, T. Weyhermüller, K. Wieghardt, C. Butzlaff, A. X. Trautwein, *J. Am. Chem. Soc.* **1996**, *118*, 12376−12390. − [24g] T. Glaser, F. Kesting, T. Beissel, E. Bill, T. Weyhermüller, W. Meyer-Klaucke, K. Wieghardt, *Inorg. Chem.* **1999**, *38*, 722−732.
[25] D. Collison, F. E. Mabbs, *J. Chem. Soc., Dalton Trans.* **1982**, 1565−1574.
[26] F. Seel, E. Müller, *Chem. Ber.* **1955**, *88*, 1747−1755.
[27] R. C. Weast, *CRC Handbook of Chemistry and Physics*, 51st ed., CRC, Ohio, **1970**.
[28] M. Davis, *Adv. Heterocycl. Chem.* **1972**, *14*, 43−98.
[29] E. A. Boudreaux, L. N. Mulay, *Theory and Applications of Molecular Paramagnetism*, Wiley, New York, **1976**.
[30] *SAINT, Version 4.050*, Siemens Analytical X-ray Instruments Inc., Madison, WI, **1995**.
[31] G. M. Sheldrick, *SADABS*, University of Göttingen, **1997**.
[32] G. M. Sheldrick, *Acta Crystallogr.* **1990**, *A46*, 467−473.
[33] G. M. Sheldrick, *SHELXL-93*, a computer program for crystal structure refinement, University of Göttingen, **1993**.
[34] H. D. Flack, *Acta Crystallogr.* **1983**, *A39*, 876−881.

Received May 18, 1999
[I99175]